Results in Physics 40 (2022) 105862

Contents lists available at ScienceDirect

Results in Physics

journal homepage: www.elsevier.com/locate/rinp

A comprehensive cost-effectiveness analysis of control of maize streak virus disease with Holling's Type II predation form and standard incidence

Baba Seidu [a,*,1], Joshua Kiddy K. Asamoah [b,*,1], Eric Neebo Wiah [c,1], Joseph Ackora-Prah [b,1]

[a] C. K. Tedam University of Technology and Applied Sciences, Navrongo, UK-0215-5321, Ghana
[b] Department of Mathematics, Kwame Nkrumah University of Science and Technology, Kumasi, Ghana
[c] Department of Mathematical Sciences, University of Mines and Technology, Takwa, Ghana

ARTICLE INFO

MSC:
34H05
34K35
65Kxx
90Cxx
93-XX

Keywords:
Epidemiology
Maize streak virus disease
Leafhopper
Cost-effectiveness analysis

ABSTRACT

Maize streak virus disease, caused by the maize streak virus, has been identified as severe vector-borne disease in Africa. In most regions of the continent, the disease is generally uncontrolled, and in epidemic years, it contributes to massive yield losses and famine. We propose a Holling-type predation functional response to explore the disease transmission. We show the sensitivity indices of various embedded parameters in the basic reproduction number. To illustrate the dynamics of the disease of the maize–leafhopper interaction, we perform a numerical simulation, and the results are graphically displayed. Incorporating four control methods (infection control, predation control, removal of infected maize plants, and insecticide application) into the basic model yields an optimal control issue. We used the Incremental Cost-Effectiveness Ratio technique to evaluate the most cost-effective combination of the four controls. We notice that the most cost-effective strategy combines the simultaneous adoption of the four controls.

Introduction

Zea mays, popular known as Maize or Corn is one of the most commonly cultivated food crops worldwide. In fact, in 2016, Maize was estimated to be second only to paddy rice in the list of most valuable crop products [1]. It is estimated that over 80% of the food consumed by humans is plant-based and hence the health of plants is key to securing the Sustainable Development Goal related to ending hunger. However, with increased international travels, climate change and continuous encroachment on forests due to the increasing populations and industrialization comes increased exposure of both plants and animals to pests and diseases. With close to 40% of annual global loss of food crop attributed to pests and diseases [2], the need for increased efforts towards fighting plant pests and diseases cannot be over-emphasized.

Maize Streak Virus Disease (MSVD) is a vector-borne disease caused by the Maize Streak Virus (MSV), affecting mostly Maize and over 80 other grasses. Following Northern Corn Leaf Blight (NCLB) and Grey Leaf Spot (GLS), MSVD comes as the third most serious disease affecting the Maize plant and even judged as the more serious than the first two in Sub-Saharan Africa [3]. The main vector of MSV is the leafhopper (predominantly, *Cicadulina mbila* Naude even though there are several other leafhopper species that serve as vectors). The vector can transmit the virus to a susceptible plant and also acquire same from an infected plant during feeding.

The role of mathematics in helping to improve our understanding of the world around us cannot be over-emphasized. Mathematics plays a major role in assessing the impact of phenomena and making projections for policy implementation. One of the areas of applications of Mathematics that has continues to receive attention is mathematical epidemiology. Mathematics has been used to successfully study the spread of various diseases and to suggest mitigating measures [4–14]. While several attempts are being made to reduce the impact of pests and disease in plants through genetic engineering and chemical application, mathematical modelling has also been shown to be a useful tool in helping to better understand the dynamics and control of infectious diseases, thus through optimal control and fractional derivatives (see for example [15–24]). Asamoah et al. [25–27] presented the ordinary differential equation and fractional models for Q fever disease in livestock. The use of mathematics to study vector-borne human, animal, vector-borne plant and environmental spread of diseases has seen some increase over the years (for reference, see the following [28, 29,29–35]). Specifically, [36] proposed an epidemic model to study the dynamics of foliar disease in maize plants and to determine the optimal

* Corresponding authors.
E-mail addresses: bseidu@cktutas.edu.gh (B. Seidu), topeljoshua@gmail.com, jkkasamoah@knust.edu.gh (J.K.K. Asamoah), enwiah@umat.edu.gh (E.N. Wiah), ackoraprahj@gmail.com (J. Ackora-Prah).

[1] The authors declare that the study was realized in collaboration with equal responsibility.

https://doi.org/10.1016/j.rinp.2022.105862
Received 10 May 2022; Received in revised form 13 July 2022; Accepted 27 July 2022
Available online 2 August 2022

strategies for control the disease. [37] proposed an SEI-SI plant-Vector model to describe the interaction between plants and MLND-vector population and observed that the contact rates among maize plants, between maize and other plants and also between maize and MLND-vectors have positive influence in driving the spread of MLND. [38] also proposed and SI-SI maize-vector ODE model to study the dynamics of Maize Streak Virus Disease. The model of [39] introduced a Pathogen compartment into the Maize–Leafhopper model to study the impact of environmental pathogen-concentration in the optimal control of MSVD and concluded that the strategy involving infection prevention and quarantine (i.e. removal and burning of infected maize plants) is the most effective strategy. The model in [38] was extended in [40] to determine the most cost-effective strategies for the control of MSVD and made the same observation as in [39] in the optimal control strategies.

While the models in [38–40] are interesting and provide useful insights into the dynamics of MSVD, it is noteworthy to mention that they described the infection of Maize plants and the predation with a composite functional form. While the predation may follow a Holling's-type functional response, the infection may not and even if it does, the composite form is over simplified and does not account for the predation of the maize by Susceptible leafhoppers. In this paper, an ordinary differential equation (ODE) model is proposed to study the spread of MSVD in Maize–Leafhopper interaction by using a Holling's-type functional response for MSVD-infection while ignoring the effect of predation. This formulation accounts for the role of the Susceptible leafhopper in the predation of maize.

The rest of the paper is structured as follows: In the next section, the mathematical model of concern is formulated. In Section "Qualitative Analysis of the MSVD Model", basic qualitative results concerning the developed model are presented. The optimal control problem is formulated in Section "The Optimal Control Model". The numerical results of the studies are given in Section "Numerical Experimentation". Finally, in Section "Conclusions" the conclusion of the study is drawn to an end.

Formulation of the mathematical model

Now, based on the model proposed in [38–40], the model is divided into maize and leafhopper population. The maize field of carrying capacity K consisting of susceptible, exposed and infected maize of sizes S_m, E_m and I_m respectively. Hence, the total maize population is given by $N_m = S_m + E_m + I_m$. An invasion of the maize field by a leafhopper population of size $N_h = S_h + I_h$ is considered, where S_h and I_h represent sizes of the susceptible and Infected leafhopper populations. Infected leafhoppers are those that have acquired the MSV and can transmit it to susceptible maize plants. The susceptible maize population grows logistically with intrinsic growth r while the leafhopper population is considered to grow at a constant rate of b susceptibles per unit time. The susceptible maize plants get exposed to MSVD through contact with infected leafhoppers at rate $\frac{\beta_{hm} I_h S_m}{N_h}$, where β_{hm} is the probability of transmission of MSVD from infected leafhopper to maize plant. The susceptible leafhoppers get infected with MSVD through contact with infected(and exposed) maize plants at rate $\frac{\beta_{mh}(E_m+I_m)S_h}{N_m}$, where β_{mh} is the probability of transmission of MSVD from infected maize plant to Susceptible leafhopper. A Holling's-Type II functional response is used to describe the rate of consumption of maize plants by leafhopper such that the rate of predation of maize is given by $\frac{aY_m N_h}{1+AY_m}$, where, Y_m represent any of the maize sub-populations, A measures the product of the attack rate and time spent processing plant by leafhopper. The use of MSVD-resistant maize varieties is assumed such that only a proportion ε of the exposed maize plants progress to the infected class at rate $\varepsilon\rho$ while the remainder reverts to the susceptible class. The parameter ρ represents the resistance maize to MSVD infection. Natural death rate of maize plants and leafhoppers are respectively taken to be μ_m and μ_h, while MSV-induced death rate in plants is α. With these assumptions, the dynamics of MSVD is described by the following set of differential equations:

$$\left.\begin{aligned}
\frac{dS_m}{dt} &= rS_m\left(1-\frac{N_m}{K}\right) + (1-\varepsilon)\,\rho\, E_m - \frac{\beta_{hm} S_m I_h}{N_h} - \frac{aS_m N_h}{1+AS_m};\\
\frac{dE_m}{dt} &= \frac{\beta_{hm} S_m I_h}{N_h} - \frac{aE_m N_h}{1+AE_m} - \left(\rho+\mu_m\right) E_m;\\
\frac{dI_m}{dt} &= \varepsilon\rho\, E_m - \frac{aI_m N_h}{1+AI_m} - \left(\alpha+\mu_m\right) I_m;\\
\frac{dS_h}{dt} &= b - \frac{\beta_{mh} S_h \left(E_m+I_m\right)}{N_m} - \mu_h S_h;\\
\frac{dI_h}{dt} &= \frac{\beta_{mh} S_h \left(E_m+I_m\right)}{N_m} - \mu_h I_h;\\
S_m(0) &\geq 0,\ E_m(0)\geq 0,\ I_m \geq (0),\ S_h(0)\geq 0,\ I_h(0)\geq 0.
\end{aligned}\right\} \quad (1)$$

In the subsequent discussions, all model variables and parameters are taken to be non-negative. Some basic qualitative properties of the model are presented in the next section.

Qualitative analysis of the MSVD model

It important to note that, all subsequent discussions of the model are considered within the region defined by Ω which can be shown to be positively invariant and thus the model (1) is mathematically and epidemiologically well-posed.

Positivity and boundedness of model solution

To determine whether model solutions are positive and constrained, the following calculation was performed for model (1).

Lemma 1. *All solution of model (1) which start in Ω remains in Ω for all $t \geq 0$.*

Also, the region $\Omega = \left\{\left(S_m,\ E_m,\ I_m\right)\times\left(S_h,\ I_h\right) \in \mathbb{R}_+^3 \times \mathbb{R}_+^2 | N_m \leq K,\ N_h \leq \frac{b}{\mu_h}\right\}$,

Proof. With reference from [41], we define $\Theta(x) = \left\{x(t) = 0, (S_m, E_m, I_m) \in \mathbb{R}^3_{\geq 0}\ and\ (S_h, I_h) \in \mathbb{R}^2_{\geq 0}\right\}, \forall x \in \left\{S_m, E_m, I_m\right\} \bigcup \left\{S_h, I_h\right\}$.

Then from model (1), we have;

$$\left\{\begin{aligned}
&\frac{dS_m}{dt}\Big|_{\Theta(S_m=0)} = (1-\varepsilon)\rho\, E_m \geq 0;\\
&\frac{dE_m}{dt}\Big|_{\Theta(E_m=0)} = \frac{\beta_{hm} S_m I_h}{N_h} \geq 0;\\
&\frac{dI_m}{dt}\Big|_{\Theta(I_m=0)} = \varepsilon\rho\, E_m \geq 0;\\
&\frac{dS_h}{dt}\Big|_{\Theta(S_h=0)} = b > 0;\\
&\frac{dI_h}{dt}\Big|_{\Theta(I_h=0)} = \frac{\beta_{mh} S_h \left(E_m+I_m\right)}{N_m} \geq 0.
\end{aligned}\right. \quad (2)$$

Now, referring to Lemma 2 of [42], indicates that any solution of model (1) is such that $(S_m, E_m, I_m) \in \mathbb{R}^3_{\geq 0}$ and $(S_h, I_h) \in \mathbb{R}^2_{\geq 0}$. Thus, the initial part of Lemma 1 is complete.

Now, since $N_m = S_m + E_m + I_m$, we have

$$\frac{dN_m}{dt} = rS_m\left(1-\frac{N_m}{K}\right) - \frac{aI_m N_h}{1+AI_m},$$
$$\frac{dN_m}{dt} \leq rN_m\left(1-\frac{N_m}{K}\right);$$
$$\therefore N_m(t) \leq \frac{KN_m(0)e^{rt}}{K + N_m(0)\left(e^{rt}-1\right)}.$$

Hence, if $0 \leq N_m(0) \leq K$, then $\limsup_{t\to+\infty} N_m(t) \leq K$.

Also, since $N_h = S_h + I_h$, we have;

$$\frac{dN_h}{dt} = b - \mu_h(S_h + I_h),$$

$$\frac{\mathrm{d}N_m}{\mathrm{d}t} \le b - \mu_h N_h.$$

Thus, $N_h(t) \le N_h(0)e^{-\mu_h t} + \frac{b}{\mu_h}\left(1 - e^{-\mu_h t}\right)$. Therefore, if $0 \le N_h(0) \le \frac{b}{\mu_h}$, then

$$\limsup_{t\to+\infty} N_h(t) \le \frac{b}{\mu_h}.$$

Hence, all solutions initiating with Ω stays in the domain of Ω. Therefore, the proof of Lemma 1 is fully complete. Hence, the proposed maize streak model (1) is mathematical and epidemiologically well-posed. □

Equilibrium points and basic reproduction number of the MSVD model

The model can be shown to have a unique MSVD-free equilibrium and possibly several endemic equilibria. A typical endemic equilibrium $\mathcal{E}^* = \left(S_m^*,\ E_m^*,\ I_m^*,\ S_h^*,\ I_h^*\right)$ of model is given by

$$\left.\begin{aligned}
S_m^* &= \frac{\left(\mu_h + \beta_{mh}\right) E_m^* \left(\mu_h\left(\rho+\mu_m\right)\left(AE_m^*+1\right)+ba\right)\left(E_m^*+I_m^*\right)}{\mu_h\left(\beta_{mh}\beta_{hm}\left(E_m^*+I_m^*\right)\left(AE_m^*+1\right)-\left(\mu_h\left(\rho+\mu_m\right)\left(AE_m^*+1\right)+ba\right)E_m^*\right)},\\
E_m^* &= \frac{\left(\left(\alpha+\mu_m\right)\left(AI_m^*+1\right)\mu_h+ba\right)I_m^*}{\mu_h\left(AI_m^*+1\right)\varepsilon\rho},\\
S_h^* &= \frac{b\left(S_m^*+E_m^*+I_m^*\right)}{\left(S_m^*+E_m^*+I_m^*\right)\mu_h+\left(E_m^*+I_m^*\right)\beta_{mh}},\\
I_h^* &= \frac{\beta_{mh} b\left(E_m^*+I_m^*\right)}{\left(\left(S_m^*+E_m^*+I_m^*\right)\mu_h+\left(E_m^*+I_m^*\right)\beta_{mh}\right)\mu_h},
\end{aligned}\right\}$$

where I_m^* can be found by substituting the endemic state variables into $\frac{dS_m}{dt} = 0$ and solving for I_m^*. The resulting equation is intractable (it is actually a 24th degree polynomial in I_m^*) and its explicit form is thus left out in this work.

The MSVD-free equilibrium is given by $\mathcal{E}_0 = \left(S_m^0,\ 0,\ 0,\ \frac{b}{\mu_h}\right)$ where S_m^0 is the solution of

$$\frac{rA}{K}\left(S_m^0\right)^2 + \left(\frac{1}{K} - A\right) rS_m^0 + \frac{ba}{\mu_h} - r = 0$$

which has a unique epidemiologically reasonable solution when $\frac{r(AK+1)^2\mu_h}{4AKab} \ge 1$.

In order to determine the basic reproduction number of the MSVD-model (1), the Next-Generation-Matrix method [43] is employed. By this method, the infected/infectious subsystem of the model is given by;

$$\left.\begin{aligned}
\frac{\mathrm{d}E_m}{\mathrm{d}t} &= \frac{\beta_{hm}S_m I_h}{N_h} - \frac{aE_mN_h}{1+AE_m} - \left(\rho+\mu_m\right)E_m;\\
\frac{\mathrm{d}I_m}{\mathrm{d}t} &= \varepsilon\rho E_m - \frac{aI_mN_h}{1+AI_m} - \left(\alpha+\mu_m\right)I_m;\\
\frac{\mathrm{d}I_h}{\mathrm{d}t} &= \frac{\beta_{mh}S_h\left(E_m+I_m\right)}{N_m} - \mu_h I_h.
\end{aligned}\right\}$$

so that the transmission and transition matrices of the model are respectively given by;

$$\mathcal{F} = \begin{bmatrix} 0 & 0 & \frac{\beta_{hm}S_m^0\mu_h}{b} \\ 0 & 0 & 0 \\ \frac{\beta_{mh}b}{\mu_hS_m^0} & \frac{\beta_{mh}b}{\mu_hS_m^0} & 0 \end{bmatrix}, \text{ and}$$

$$\mathcal{V} = \begin{bmatrix} \frac{ba}{\mu_h}+\rho+\mu_m & 0 & 0 \\ -\varepsilon\rho & \frac{ba}{\mu_h}+\alpha+\mu_m & 0 \\ 0 & 0 & \mu_h \end{bmatrix}$$

The Next-generation matrix of the model is thus given by $\mathcal{F}\mathcal{V}^{-1}$ in Box I. The basic reproduction number determined by the spectral radius of $\mathcal{F}\mathcal{V}^{-1}$ is given by

$$\mathcal{R}_0 = \sqrt{\frac{\beta_{mh}\beta_{hm}\left(ba+\mu_h\left(\varepsilon\rho+\alpha+\mu_m\right)\right)}{\left(ba+\mu_h\left(\rho+\mu_m\right)\right)\left(ba+\mu_h\left(\alpha+\mu_m\right)\right)}}.$$

The basic reproduction number measures the average number of MSVD infections that will result due to the introduction of a single infectious leafhopper into an initially MSVD-free maize field.

Local stability of MSVD-free equilibrium $\mathcal{E}_0$

The Jacobian of the model at $\mathcal{E}_0$ is given by $\mathcal{J}\left(\mathcal{E}_0\right)$ in Box II where $\mathcal{J}_{11} = r\left(1-2\frac{S_m^0}{K}\right) - \frac{ba}{\mu_h\left(AS_m^0+1\right)^2}$, which has two of its eigenvalues given by $-\mu_h$ and $\mathcal{J}_{11}$ and the rest of the eigenvalues are zeros of the characteristic equation given by

$$\lambda^3 + \Phi_2\lambda^2 + \Phi_1\lambda + \Phi_0 = 0, \tag{3}$$

where

$$\begin{aligned}
\Phi_2 &= \frac{2\,ab}{\mu_h} + \alpha + \rho + \mu_h + 2\,\mu_m,\\
\Phi_1 &= 2ab + \mu_h\left(\rho+\alpha+2\,\mu_m\right) + \left(ba+\mu_h\left(\rho+\mu_m\right)\right)\left(ba+\mu_h\left(\alpha+\mu_h\right)\right)\\
&\quad\times\left(\frac{1}{\mu_h^2} - \frac{\mathcal{R}_0^2}{ba+\mu_h\left(\varepsilon\rho+\alpha+\mu_m\right)}\right),\\
\Phi_0 &= \left(ba+\mu_h\left(\rho+\mu_m\right)\right)\left(ba+\mu_h\left(\alpha+\mu_m\right)\right)\left(1-\mathcal{R}_0^2\right).
\end{aligned}$$

The zeros of (3) have negative eigenvalues if $\Phi_0 > 0$ (or equivalently $\mathcal{R}_0 \le 1$) and $\Phi_1 - \frac{\Phi_0}{\Phi_2} > 0$. The importance for $\mathcal{R}_0 \le 1$ indicates that the disease cannot establish itself in the maize population [44]. The following mathematical result is thus obtained.

Theorem 1. *The MSVD-free equilibrium of the model is locally asymptotically stable whenever $\mathcal{R}_0 \le 1$, $\Phi_1 - \frac{\Phi_0}{\Phi_2} > 0$ and $\frac{2S_m^0}{K} + \frac{ba}{r\mu_h\left(AS_m^0+1\right)^2} > 1$.*

Theorem 1 indicates that $\mathcal{R}_0 \le 1$ is not sufficient for disease eradication, since other conditions need to be satisfied in addition to $\mathcal{R}_0 \le 1$ for the MSVD-free equilibrium to be locally asymptotically stable. Therefore, the model cannot exhibit forward bifurcation unless the conditions in this theorem are satisfied.

Sensitivity analysis of $\mathcal{R}_0$

The motive here is to find parameters that are most sensitive to the spread of the maize streak virus disease under Holling's Type II predation form and standard incidence infection. It can be seen that most of the parameters in the proposed model are captured in $\mathcal{R}_0$. Therefore, one can use the normalized forward-sensitivity index measures to test for the local sensitiveness of the parameters in $\mathcal{R}_0$ and the Latin hypercube sampling (LHS) to test for the global sensitiveness of the parameters in $\mathcal{R}_0$. The normalized forward-sensitivity index is defined as

$$\Lambda_{p_i^*}^{\mathcal{R}_0} = \frac{\partial\mathcal{R}_0}{\partial p_i^*} \times \frac{p_i^*}{\mathcal{R}_0}, \tag{4}$$

where, p_i^* represent the various parameters in $\mathcal{R}_0$.

If $D_1 = ba + \mu_h\left(\varepsilon\rho+\alpha+\mu_m\right)$, $D_2 = ba + \mu_h\left(\rho+\mu_m\right)$ and $D_3 = ba + \mu_h\left(\alpha+\mu_m\right)$, then the sensitivity indexes of the parameters are given in Box III: The above normalized forward-sensitivity analysis shows that, β_{hm}, the probability of transmission of MSVD from infected leafhopper to maize plant and β_{mh}, the probability of transmission of MSVD from infected maize plant to susceptible leafhopper contributes positively to the spread of the disease in the ecosystem. We can also see that farmers who use MSVD-resistant maize varieties reduce the spread of the disease because the product of $\varepsilon\rho$ gives a negative sensitive index. The natural death rate of maize plants, μ_m, leafhoppers, μ_h and the

$$\mathcal{F}\mathcal{V}^{-1} = \begin{bmatrix} 0 & 0 & \frac{\beta_{hm} S_m}{b} \\ 0 & 0 & 0 \\ \frac{\beta_{mh} b}{S_m\left(ba+\mu_h\left(\rho+\mu_m\right)\right)} + \frac{\beta_{mh} b \mu_h \rho\, \varepsilon}{S_m(ba+\mu_h(\rho+\mu_m))(ba+\mu_h(\alpha+\mu_m))} & \frac{\beta_{mh} b}{S_m\left(ba+\mu_h\left(\alpha+\mu_m\right)\right)} & 0 \end{bmatrix}.$$

Box I.

$$\mathcal{J}\left(\mathcal{E}_0\right) = \begin{bmatrix} \mathcal{J}_{11} & -\frac{rS_m^0}{K} + (1-\varepsilon)\rho & -\frac{rS_m^0}{K} & -\frac{aS_m}{AS_m^0+1} & -\frac{\beta_{hm} S_m^0 \mu_h}{b} - \frac{aS_m^0}{AS_m^0+1} \\ 0 & -\frac{ba}{\mu_h} - \rho - \mu_m & 0 & 0 & \frac{\beta_{hm} S_m^0 \mu_h}{b} \\ 0 & \varepsilon\rho & -\frac{ba}{\mu_h} - \alpha - \mu_m & 0 & 0 \\ 0 & -\frac{\beta_{mh} b}{\mu_h S_m^0} & -\frac{\beta_{mh} b}{\mu_h S_m^0} & -\mu_h & 0 \\ 0 & \frac{\beta_{mh} b}{\mu_h S_m^0} & \frac{\beta_{mh} b}{\mu_h S_m^0} & 0 & -\mu_h \end{bmatrix},$$

Box II.

$$\Lambda_{\beta_{mh}}^{\mathcal{R}_0} = \frac{1}{2}, \qquad \Lambda_{\beta_{hm}}^{\mathcal{R}_0} = \frac{1}{2}, \qquad \Lambda_{a}^{\mathcal{R}_0} = \frac{ab}{2}\left(\frac{1}{D_1} - \frac{1}{D_2} - \frac{1}{D_3}\right),$$

$$\Lambda_{b}^{\mathcal{R}_0} = \frac{ab}{2}\left(\frac{1}{D_1} - \frac{1}{D_2} - \frac{1}{D_3}\right), \qquad \Lambda_{\varepsilon}^{\mathcal{R}_0} = \frac{\mu_h \varepsilon \rho}{2D_1}, \qquad \Lambda_{\mu_h}^{\mathcal{R}_0} = \frac{\mu_h}{2}\left(\frac{(\varepsilon\rho+\alpha+\mu_m)}{D_1} - \frac{(\rho+\mu_m)}{D_2} - \frac{(\alpha+\mu_m)}{D_3}\right),$$

$$\Lambda_{\alpha}^{\mathcal{R}_0} = \frac{\alpha\mu_h}{2}\left(\frac{1}{D_1} - \frac{1}{D_3}\right), \qquad \Lambda_{\rho}^{\mathcal{R}_0} = \frac{\mu_h \rho}{2}\left(\frac{\varepsilon}{D_1} - \frac{1}{D_2}\right), \qquad \Lambda_{\mu_m}^{\mathcal{R}_0} = \frac{\mu_h \mu_m}{2}\left(\frac{1}{D_1} - \frac{1}{D_2} - \frac{1}{D_3}\right).$$

Box III.

MSV-induced death rate in plants, α, respectively decrease the spread of the disease. It is also noticed that the conversion rate of infected leafhopper a and the leafhopper population increased through birth and immigration b have the same magnitude in reducing the spread of the disease. Further discussion of this is done in Section "Numerical Sensitivity Indices".

Existence of bifurcation

It is easy to show that if $\beta_{mh}^* = \frac{(ba+\mu_h(\alpha+\mu_m))(ba+\mu_h(\rho+\mu_m))}{(ba+\mu_h(\varepsilon\rho+\alpha+\mu_m))\beta_{hm}}$ is chosen as a bifurcation parameter, then the Jacobian of the Model (1) will have a simple zero eigenvalue. This implies that the centre manifold theory as described in [45] can be used to study the stability of the MSVD-free equilibrium point. By this theory, the stability of the equilibria of the MSVD model can be completely characterized by the bifurcation coefficients **a** and **b** given by

$$\mathbf{a} = \sum_{i,j,k=1}^{n} v_k w_i w_j \frac{\partial^2 f_k}{\partial x_i \partial x_j}\left(\mathcal{E}_0, \beta_{mh}^*\right), \quad \text{and } \mathbf{b} = \sum_{i,k=1}^{n} v_k w_i \frac{\partial^2 f_k}{\partial x_i \partial \beta_1}\left(\mathcal{E}_0, \beta_{mh}^*\right),$$

where **w** and **v** are the right and left eigenvalues of the Jacobian of Model (1) at the MSVD-free equilibrium point and $f(x)$ is the right-hand side of the model with $x_1 = S_m$, $x_2 = E_m$, $x_3 = I_m$, $x_4 = S_h$ and $x_5 = I_h$. The right and left eigenvalues of $\mathcal{J}\left(\mathcal{E}_0\right)$ are given by w in Box IV and $v = \begin{pmatrix} 0 & v_2 & \frac{\beta_{mh}\beta_{hm} v_2}{ba+\alpha\mu_h+\mu_h\mu_m} & 0 & \frac{\beta_{hm} S_m^0 v_2}{b} \end{pmatrix}^T$ with,

$$\eta = \left(\frac{\rho(1-\varepsilon) - \left(\frac{S_m^0 r}{K} + \beta_{\mathrm{mh}}^* \beta_{\mathrm{hm}}\right)\frac{\left(\rho\varepsilon + S_h^0 a + \alpha + \mu_m\right)}{\mu_h\left(S_h^0 a + \alpha + \mu_m\right)}}{r\left(\frac{2S_m^0}{K} - 1\right) + \frac{ab}{\mu_h\left(A S_m^0 + 1\right)^2}}\right) w_2$$

where w_2 and v_2 are chosen such that $w \bullet v = 1$. The bifurcation coefficients are therefore obtained as

$$\mathbf{a} = 2\left(\mathbf{A}_1 - \mathbf{A}_2\right) w_2^2 v_2 \text{ and } \mathbf{b} = \frac{\beta_{hm}\left[ba + \mu_h\left(\varepsilon\rho + \alpha + \mu_m\right)\right] w_2 v_2}{\mu_h\left(ba + \mu_h\left(\alpha + \mu_m\right)\right)},$$

where

$$\mathbf{A}_1 = A S_h^0 a + \frac{A S_h^0 a \beta_{\mathrm{hm}} \beta_{\mathrm{mh}} \rho^2 \varepsilon^2}{\mu_h\left(S_h^0 a + \alpha + \mu_m\right)^3},$$

$$\mathbf{A}_2 = \mathbf{A}_2 = \frac{\beta_{\mathrm{hm}}\beta_{\mathrm{mh}}}{S_m^0}\left[\frac{1 - \eta\left(1+\mu_h\right)}{\mu_h} + \frac{\beta_{\mathrm{mh}}(1+\varepsilon)\left(\rho\varepsilon + S_h^0 a + \alpha + \mu_m\right)}{{\mu_h}^2\left(S_h^0 a + \alpha + \mu_m\right)} + \frac{2\rho\varepsilon}{\mu_h\left(S_h^0 a + \alpha + \mu_m\right)} + \frac{\rho^2\varepsilon^2}{\mu_h\left(S_h^0 a + \alpha + \mu_m\right)^2}\right].$$

Clearly, $\mathbf{b} > 0$ and hence by Theorem 4.1 of [45], the following result is established.

Theorem 2. *The MSVD-Model (1) near $\mathcal{R}_0 = 1$ exhibits a forward bifurcation whenever, $\mathbf{A}_1 > \mathbf{A}_2$. Also, the Model exhibits a backward bifurcation whenever $\mathbf{A}_1 < \mathbf{A}_2$.*

$$w = \left[\begin{array}{ccccc} \eta\, w_2 & w_2 & \dfrac{\varepsilon\, \rho\, w_2 \mu_h}{ba + \mu_h \left(\alpha + \mu_m\right)} & -\dfrac{w_2 \beta_{mh} \left(ba + \mu_h \left(\varepsilon\, \rho + \alpha + \mu_m\right)\right) b}{{\mu_h}^2 \left(ba + \mu_h \left(\alpha + \mu_m\right)\right) S_m^0} & \dfrac{w_2 \beta_{mh} \left(ba + \mu_h \left(\varepsilon\, \rho + \alpha + \mu_m\right)\right) b}{{\mu_h}^2 \left(ba + \mu_h \left(\alpha + \mu_m\right)\right) S_m^0} \end{array}\right],$$

Box IV.

The optimal control model

The aim of the section is to propose a problem with which the spread of MSVD can be optimized. Thus, the attempt to find the most cost-effective strategy to curtail the spread of MSVD with the minimal cost is made. In order to do this, the following controls are introduced into the model (1):

(i) $u_1(t)$ is the control strategy to reduce infection of maize plant by leafhopper,
(ii) $u_2(t)$ is the control strategy to reduce predation of maize plant.
(iii) $u_3(t)$ is the control strategy involving removal of infected maize from the field. This goes a long way to also reduce the infection of leafhopper by infected maize.
(iv) $u_4(t)$ is the control for insecticide application to kill leafhoppers.

With these controls, the MSVD model in (1), is modified into the following model:

$$\left.\begin{aligned}
\frac{\mathrm{d}S_m}{\mathrm{d}t} &= rS_m\left(1-\frac{N_m}{K}\right) + (1-\varepsilon)\,\rho\, E_m \\
&\quad - \frac{(1-u_1(t))\beta_{hm}S_m I_h}{N_h} - \frac{a(1-u_2(t))S_m N_h}{1+AS_m};\\
\frac{\mathrm{d}E_m}{\mathrm{d}t} &= \frac{(1-u_1(t))\beta_{hm}S_m I_h}{N_h} - \frac{a(1-u_2(t))E_m N_h}{1+AE_m} - \left(\rho+\mu_m\right)E_m;\\
\frac{\mathrm{d}I_m}{\mathrm{d}t} &= \varepsilon\rho\, E_m - \frac{a(1-u_2(t))I_m N_h}{1+AI_m} - \left(u_3(t)+\alpha+\mu_m\right)I_m;\\
\frac{\mathrm{d}S_h}{\mathrm{d}t} &= b - \frac{(1-u_3(t))\beta_{mh}S_h\left(E_m+I_m\right)}{N_m} - \left(u_4(t)+\mu_h\right)S_h;\\
\frac{\mathrm{d}I_h}{\mathrm{d}t} &= \frac{(1-u_3(t))\beta_{mh}S_h\left(E_m+I_m\right)}{N_m} - \left(u_4+\mu_h\right)I_h,
\end{aligned}\right\} \quad (5)$$

with the initial conditions stated in (1) and $u_i \in \mathcal{U}$, where $\mathcal{U}$ is the set of admissible controls.

Now, the objectives – which are to minimize the infection at the end of the interval $[0,\ t_f]$, and to minimize the cost incurred over the application of the controls – will be achieved by minimizing the objective functional

$$\mathcal{I}(u) = \int_0^T \left[\sum_{i=1}^{4}\frac{1}{2}\omega_i u_i^2 + B_m I_m + B_h(S_h+I_h)\right]\mathrm{d}t, \quad (6)$$

where T is the final time, B_m and B_h are balancing constant coefficients of the infected maize and infected leafhopper respectively while ω_i are weight coefficients that depends on the cost of application of each control measure. Thus, the goal here is to minimize $\mathcal{I}(u)$ subject to (5).

The Pontryagin's Optimality Principle (POP) helps us to devise the necessary conditions for optimal controls $u_i^* \in U$ presented by Lenhart and Workman [46]. But before we show these conditions, we have the following existence theorem for the said controls u_i^*.

Theorem 3. *There exists $u_i^* \in U$, with the corresponding state variables $S_m^*, E_m^*, I_m^*, S_h^*$ and I_h^*, such that $\mathcal{I}(u_i^*) \le \mathcal{I}(u_i)$ for all $u_i \in U$.*

The proof of Theorem 3 follows directly from the existence theorem for the solutions of such problem as shown in [47]

Notation. Hereinafter, we denote $x = (S_m, E_m, I_m, S_h, I_h)$, $u = (u_1, u_2, u_3, u_4)$, $f = (f_{S_m}, f_{E_m}, f_{I_m}, f_{S_h}, f_{I_h})^T$, where $f_{S_m}, f_{E_m}, f_{I_m}, f_{S_h}$, and f_{I_h} denote the right-hand side of system (1), respectively. Also, we let $\lambda = (\lambda_1, \lambda_2, \lambda_3, \lambda_4, \lambda_5)^T$ be the adjoint state.

Now, from Pontryagin's optimality principle, we define the Hamiltonian $H(u,\lambda,x,t)$ as

$$H(u,\lambda,x,t) = \sum_{i=1}^{4}\frac{1}{2}\omega_i u_i^2 + B_m I_m + B_h(S_h+I_h) + \lambda \times f.$$

Theorem 4 (*Necessary Conditions*).. *If $u^* \in U^2$ are the optimal control for (6), with corresponding optimal state x^*, then the adjoint variable λ exists and satisfies $\dot{\lambda} = -\partial_x H$, with transversality conditions $\lambda_i(t_f) = 0, i = 1,\dots,5$. Furthermore, the optimal controls u^* are characterized as follows*

$$\begin{cases} u^* = 0 & \text{if} \quad \partial_u H > 0,\\ u^* \in (0,1)^2 & \text{if} \quad \partial_u H = 0,\\ u^* = 1 & \text{if} \quad \partial_u H < 0,\end{cases}$$

and the state variables x^* satisfy (5) subject to (6).

The necessary conditions that an optimal solution must satisfy the maximum principle of [48]. This principle converts the model of Eqs. (5) and (6) into a problem of minimizing point-wise a Hamiltonian, H, with respect to $u_i(t)$ as:

$$H(u,\lambda,x,t) = \sum_{i=1}^{4}\frac{1}{2}\omega_i u_i^2 + B_m I_m + B_h(S_h+I_h) + \lambda_1\frac{\mathrm{d}S_m}{\mathrm{d}t} + \lambda_2\frac{\mathrm{d}E_m}{\mathrm{d}t} + \lambda_3\frac{\mathrm{d}I_m}{\mathrm{d}t} + \lambda_4\frac{\mathrm{d}S_h}{\mathrm{d}t} + \lambda_5\frac{\mathrm{d}I_h}{\mathrm{d}t},$$

which can be written as

$$\left.\begin{aligned}
H(u,\lambda,x,t) = \quad & \sum_{i=1}^{4}\frac{1}{2}\omega_i u_i^2 + B_m I_m + B_h(S_h+I_h)\\
& + \lambda_1[rS_m\left(1-\frac{N_m}{K}\right) + (1-\varepsilon)\,\rho\, E_m\\
& - \frac{(1-u_1(t))\beta_{hm}S_m I_h}{N_h} - \frac{a(1-u_2(t))S_m N_h}{1+AS_m}]\\
& + \lambda_2[\frac{(1-u_1(t))\beta_{hm}S_m I_h}{N_h}\\
& - \frac{a(1-u_2(t))E_m N_h}{1+AE_m} - \left(\rho+\mu_m\right)E_m]\\
& + \lambda_3[\varepsilon\rho\, E_m - \frac{a(1-u_2(t))I_m N_h}{1+AI_m}\\
& - \left(u_3(t)+\alpha+\mu_m\right)I_m]\\
& + \lambda_4[b - \frac{(1-u_3(t))\beta_{mh}S_h\left(E_m+I_m\right)}{N_m}\\
& - \left(u_4(t)+\mu_h\right)S_h]\\
& + \lambda_5[\frac{(1-u_3(t))\beta_{mh}S_h\left(E_m+I_m\right)}{N_m}\\
& - \left(u_3(t)+\mu_h\right)I_h],
\end{aligned}\right\} \quad (7)$$

where λ_1, λ_2, λ_3, λ_4 and λ_5 are the adjoint variables or co-state variables. From Eq. (7), the following adjoint equations can be obtained by taking $\frac{\lambda_i}{t} = -\frac{\partial H}{\partial x_i}$ where $x = \left(S_m,\ E_m,\ I_m,\ S_h,\ I_h\right)$ (see Eq. (8) given in Box V): with transversality condition (or boundary condition): $\lambda_i(T) = 0, i = 1,\ 2\dots 5$.

The optimal controls are characterized by

$$u_i^* = \max\left\{u_i^{\min},\ \min\left\{u_i^{\max},\ \phi_i\right\}\right\},\ \forall i = 1, 2, 3, 4.$$

$$\left.\begin{aligned}
\frac{\mathrm{d}\lambda_1}{\mathrm{d}t} &= -\lambda_1\left[r\left(1-\frac{2\,S_m+E_m+I_m}{K}\right)-\frac{a\left(1-u_2\right)N_h}{\left(AS_m+1\right)^2}\right]+\frac{\left(1-u_1\right)\beta_{hm}I_h\left(\lambda_1-\lambda_2\right)}{N_h}+\frac{\left(1-u_3\right)\beta_{mh}S_h\left(E_m+I_m\right)\left(\lambda_5-\lambda_4\right)}{N_m^2},\\
\frac{\mathrm{d}\lambda_2}{\mathrm{d}t} &= \frac{\lambda_1 rS_m}{K}+\left[\frac{a\left(1-u_2\right)N_h}{\left(AE_m+1\right)^2}+\mu_m\right]\lambda_2+\frac{\left(1-u_3\right)\beta_{mh}S_hS_m\left(\lambda_4-\lambda_5\right)}{N_m^2}+\rho\left[\lambda_2-\lambda_1+\varepsilon\left(\lambda_1-\lambda_3\right)\right],\\
\frac{\mathrm{d}\lambda_3}{\mathrm{d}t} &= -B_m+\frac{\lambda_1 rS_m}{K}+\lambda_3\left[\frac{a\left(1-u_2\right)\left(S_h+I_h\right)}{\left(AI_m+1\right)^2}+u_3+\alpha+\mu_m\right]+\frac{\left(1-u_3\right)\beta_{mh}S_hS_m\left(\lambda_4-\lambda_5\right)}{N_m^2},\\
\frac{\mathrm{d}\lambda_4}{\mathrm{d}t} &= -B_h+\frac{\left(1-u_1\right)\beta_{hm}S_mI_h\left(\lambda_2-\lambda_1\right)}{N_h^2}+a\left(1-u_2\right)\left[\frac{S_m\lambda_1}{AS_m+1}+\frac{E_m\lambda_2}{AE_m+1}+\frac{I_m\lambda_3}{AI_m+1}\right]+\lambda_4\left(u_4+\mu_h\right),\\
&\quad+\frac{\left(1-u_3\right)\beta_{mh}\left(E_m+I_m\right)\left(\lambda_4-\lambda_5\right)}{N_m}\\
\frac{\mathrm{d}\lambda_5}{\mathrm{d}t} &= -B_h+\frac{\left(1-u_1\right)\beta_{hm}S_mS_h\left(\lambda_1-\lambda_2\right)}{N_h^2}+a\left(1-u_2\right)\left[\frac{S_m\lambda_1}{AS_m+1}+\frac{E_m\lambda_2}{AE_m+1}+\frac{I_m\lambda_3}{AI_m+1}\right]+\lambda_5\left(u_4+\mu_h\right).
\end{aligned}\right\} \quad (8)$$

Box V.

Table 1
Description and baseline values of model parameter used in numerical simulations.

Parameter	Description	Baseline value	Source
b	Incremental rate of susceptible leafhopper	20	Assumed
β_{hm}	Probability of transmission of MSVD from infected leafhopper to maize plant	0.45	[49]
β_{mh}	Probability of transmission of MSVD from infected maize plant to Leafhopper	0.04	[49]
μ_m	Natural death rate of maize plants	1/120	[50]
μ_h	Natural death rate of leafhoppers	1/33	[51]
a	Conversion rate of Infected leafhopper	0.45	[52]
ρ	Resistance maize to MSVD infection	0.001	Assumed
ε	Proportion of exposed maize	0.50	Assumed
α	MSV-induced death rate in plants	0.001	Assumed
r	Intrinsic growth rate of Maize	0.0005	[52,53]
A	Product of the attack rate and time spent processing plant by leafhopper	0.4	[52]
K	Carrying capacity	10,000	[52]

where ϕ_i are obtained by solving $\frac{\partial H}{\partial u_i(t)} = 0$ and are given by

$$\begin{aligned}
\phi_1 &= \frac{\beta_{hm}S_mI_h\left(\lambda_2-\lambda_1\right)}{N_h\omega_1};\\
\phi_2 &= -\frac{aN_h}{\omega_2}\left[\frac{S_m\lambda_1}{AS_m+1}+\frac{E_m\lambda_2}{AE_m+1}+\frac{I_m\lambda_3}{AI_m+1}\right];\\
\phi_3 &= \frac{1}{\omega_3}\left[I_m\lambda_3-\frac{\beta_{mh}S_h\left(E_m+I_m\right)}{N_m}\left(\lambda_4-\lambda_5\right)\right];\\
\phi_4 &= \frac{1}{\omega_4}[\lambda_4S_h+\lambda_5I_h].
\end{aligned}$$

In this paper, the minimum and maximum control bounds are taken to be 0 and 1 respectively to represent non-application and 100% application respectively. The characterizations of the optimal controls are thus given by:

$$u_i^* = \begin{cases} 0 & \text{if} \quad \phi_i \le 0, \\ \phi_i & \text{if} \quad 0 < \phi_i < 1, \quad \forall\, i = 1,\ 2,\ 3,\ 4. \\ 1 & \text{if} \quad \phi_i \ge 1, \end{cases}$$

Numerical experimentation

In this section, using the Runge–Kutta method of order four, numerical experiments are conducted on the model to illustrate or confirm the analytical results and also to further study the impact of various model parameters on the spread of MSVD. Also, using the forward–backward sweep scheme [46], the optimal control problem is numerically simulated in order to illustrate the cost-effectiveness of various combinations of the controls. Unless otherwise stated, the baseline parameter values presented in Table 1 are used in the simulations.

Numerical sensitivity indices

Using the parameter values in Table 1, the local normalized sensitivity indices of $\mathcal{R}_0$ are obtained and presented in Table 2. Fig. 1(a) shows the global sensitivity indexes of the parameters in $\mathcal{R}_0$, which is in agreement with the directional flow of the local sensitivity analysis. From Fig. 1(a) we see that the most positive sensitivity parameter in the basic reproduction number is β_{mh}, the probability of transmission of MSVD from infected maize plant to susceptible leafhopper followed by β_{hm}, the probability of transmission of MSVD from infected leafhopper to maize plants. Likewise, we see that the most negative sensitivity parameter in the basic reproduction number is b, the incremental rate of susceptible leafhopper, followed by a, the conversion rate of infected leafhopper. On the other hand, the uncertainty analysis (UA) in Fig. 1(b) shows that the range of the R_0 is approximately [0.03 – 0.06], though most of the outputs are concentrated in low values ([0.03 – 0.047]).

Numerical simulations without controls

Simulating the model (1) with varying β_{hm} values while holding all other baseline parameter values constant produces the results shown in Fig. 2(d). Thus, in Fig. 2(d) we noticed that a reduction in the probability of transmission of MSVD from infected leafhoppers to maize plants increases the number of healthy maize plants, thereby reducing the number of infected maize and infected leafhoppers. Simulating the model (1) with varying β_{mh} values while holding all other baseline parameter values constant produces the results shown in Fig. 3(d). Thus, in Fig. 3(d) we noticed that a reduction in the probability of transmission of MSVD from infected maize to leafhoppers slightly increases the number of healthy maize plants, thereby slightly reducing

Table 2
Normalized forward-sensitivity indexes of $\mathcal{R}_0$.

Parameter	b	μ_m	β_{hm}	μ_h	a	β_{mh}	ρ	ϵ	α
Value	−0.4985	−0.0014	0.5000	−0.0015	−0.4985	0.5000	−0.0001	0.0001	-2.8×10^{-8}

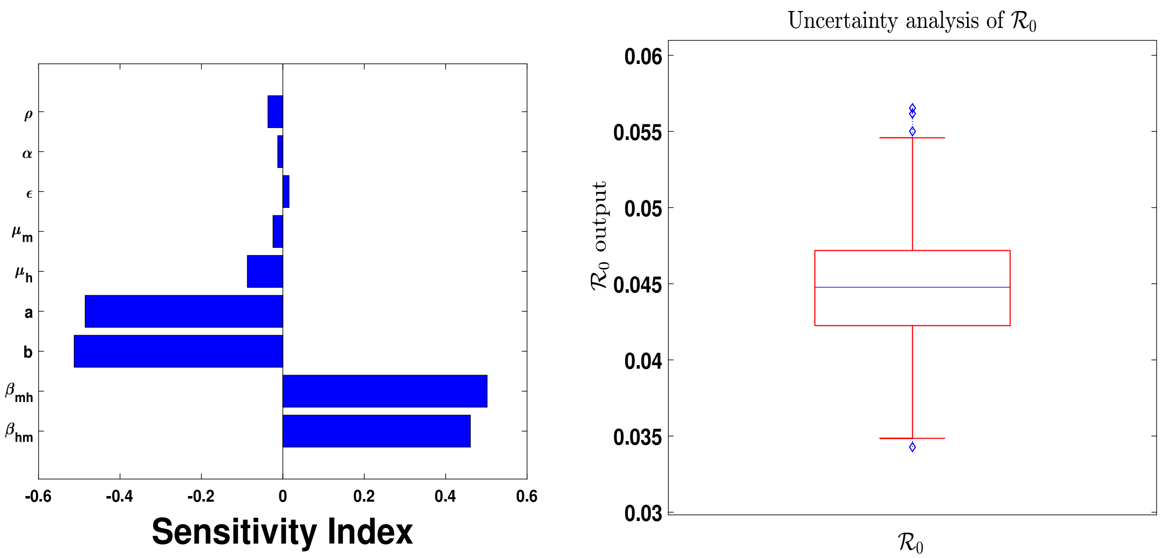

(a) PRCC plot for maize strike virus disease.

(b) The box plot of $\mathcal{R}_0$.

Fig. 1. Global sensitivity and uncertainty analysis of $\mathcal{R}_0$.

the number of infected maize. Therefore, comparing 2(d) with 3(d), it indicates that to have a higher yield of maize, all effort should be pushed towards the reduction of the probability of transmission of MSVD from infected leafhoppers to maize.

Numerical simulations of the optimal control problem

In this section, the optimal control problem is simulated to determine the cost-effectiveness of the various combinations of the controls. In order to achieve this, the optimal control problem is solved for the various combinations of the controls, while calculating the total number of maize plant infections averted and the total cost incurred (see Table 3). The total maize plant infections averted is the total size of the maize plants over the period of simulation without controls minus that with controls. Using the forward backward sweep, the optimal control model is simulated with the following initial conditions and weights:

$$S_m(0) = 12000, E_m(0) = 100, I_m(0) = 0, S_h(0) = 100,$$
$$I_h(0) = 10 w_1 = 5, w_2 = 5, w_3 = 5, w_4 = 5, B_m = 2, \text{ and } B_h = 1.$$

The 15 possible combinations of the controls are as follows:

Control Strategy ($CS1$): $u_1(t)$ is the control strategy to reduce infection of maize plant by leafhopper.

Control Strategy ($CS2$): $u_2(t)$ is the control strategy to reduce predation of maize plant.

Control Strategy ($CS3$): $u_3(t)$ is the control strategy involving removal of infected maize from the field.

Control Strategy ($CS4$): $u_4(t)$ is the control for insecticide application to kill leafhoppers.

Control Strategy ($CS5$): the use of the control strategy to reduce infection of maize plant by leafhopper $u_1(t)$, and the control strategy to reduce predation of maize plant $u_2(t)$ only.

Control Strategy ($CS6$): the use of the control strategy to reduce infection of maize plant by leafhopper $u_1(t)$, and the control strategy involving removal of infected maize from the field $u_3(t)$ only.

Control Strategy ($CS7$): the use of the control strategy to reduce infection of maize plant by leafhopper $u_1(t)$, and the control for insecticide application to kill leafhoppers $u_4(t)$ only.

Control Strategy ($CS8$): the use of the control strategy to reduce predation of maize plant $u_2(t)$, and the control strategy involving removal of infected maize from the field $u_3(t)$ only.

Control Strategy ($CS9$): the use of the control strategy to reduce predation of maize plant $u_2(t)$, and the control for insecticide application to kill leafhoppers $u_4(t)$, only at time t.

Control Strategy ($CS10$): the use of the control strategy involving removal of infected maize from the field $u_3(t)$, the control for insecticide application to kill leafhoppers $u_4(t)$, only at time t.

Control Strategy ($CS11$): the use of the control strategy to reduce infection of maize plant by leafhopper $u_1(t)$, the control strategy to reduce predation of maize plant $u_2(t)$, and the control strategy involving removal of infected maize from the field $u_3(t)$ only.

Control Strategy ($CS12$): the use of the control strategy to reduce infection of maize plant by leafhopper $u_1(t)$, the control strategy to reduce predation of maize plant $u_2(t)$, the control for insecticide application to kill leafhoppers $u_4(t)$, only at time t.

Control Strategy ($CS13$): the use of the control strategy to reduce infection of maize plant by leafhopper $u_1(t)$, the control strategy involving removal of infected maize from the field $u_3(t)$, the

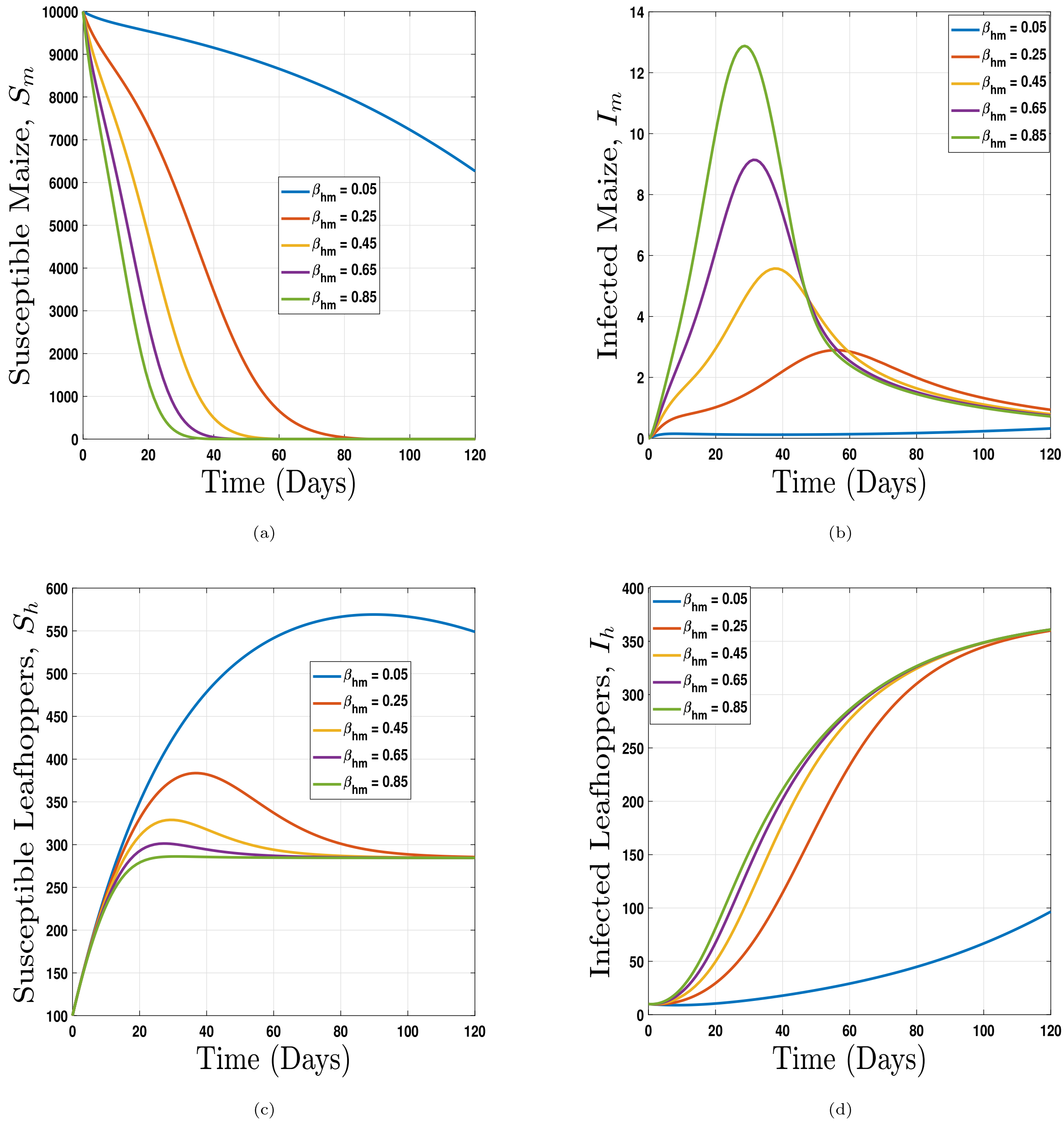

Fig. 2. Time Series plots of the effect of varying β_{hm}, the probability of Leafhopper-to-Maize transmission of MSVD.

control for insecticide application to kill leafhoppers $u_4(t)$, only at time t.

Control Strategy $(CS14)$: the use of the control strategy to reduce predation of maize plant $u_2(t)$, the control strategy involving removal of infected maize from the field $u_3(t)$, the control for insecticide application to kill leafhoppers $u_4(t)$, only at time t.

Control Strategy $(CS15)$: the use of all controls, $u_1(t), u_2(t), u_3(t), u_4(t)$.

From Table 3, the cost-effectiveness for each of the control strategies can be calculated. The cost-effectiveness analysis can then be done using the incremental cost-effectiveness ratio (ICER), which has been used in most optimal control research [54,55] to determine the best and most effective control strategy at a minimal cost. The incremental cost-effectiveness ratio (ICER) assesses the variations between the costs and health benefits of distinct intervention options vying for the same constrained resources [56]. Assuming strategies p and q as two main control intervention strategies, then ICER of p^* relative to q^* is expressed as

$$\text{ICER}(p^*, q^*) = \frac{\text{Total costs in strategies } p^* \text{ minus Total costs in strategies } q^*}{\text{Benefits in strategies } p^* \text{ minus Benefits in strategies } q^*}.$$

where p^* and q^* are often chosen such that q^* has the least cost than p^*. If ICER(p^*, q^*) is lower that the cost-to-benefit ratio of q^* then p^* is said to be more cost-effective that the q^*, otherwise q^* is most cost-effective. Alternatively, if p^* and q^* are chosen such that q^* has the most benefit, then if ICER(p^*, q^*) is lower than the cost-to-benefit ratio of q^* then p^* is said to be more cost-effective that the q^*, otherwise q^* is most cost-effective. In this paper, the benefit of implementing strategies is taken as the total MSVD-infection of maize averted.

Using the data in Table 3, the ICER are calculated for the various control strategies in the following categories:

Group A: Single controls (CS_1 to CS_4),
Group B: Double control combinations (CS_5 to CS_{10}),
Group C: Three control combinations (CS_{11} to CS_{14}), and
Group D: Four control combinations (CS_{15}).

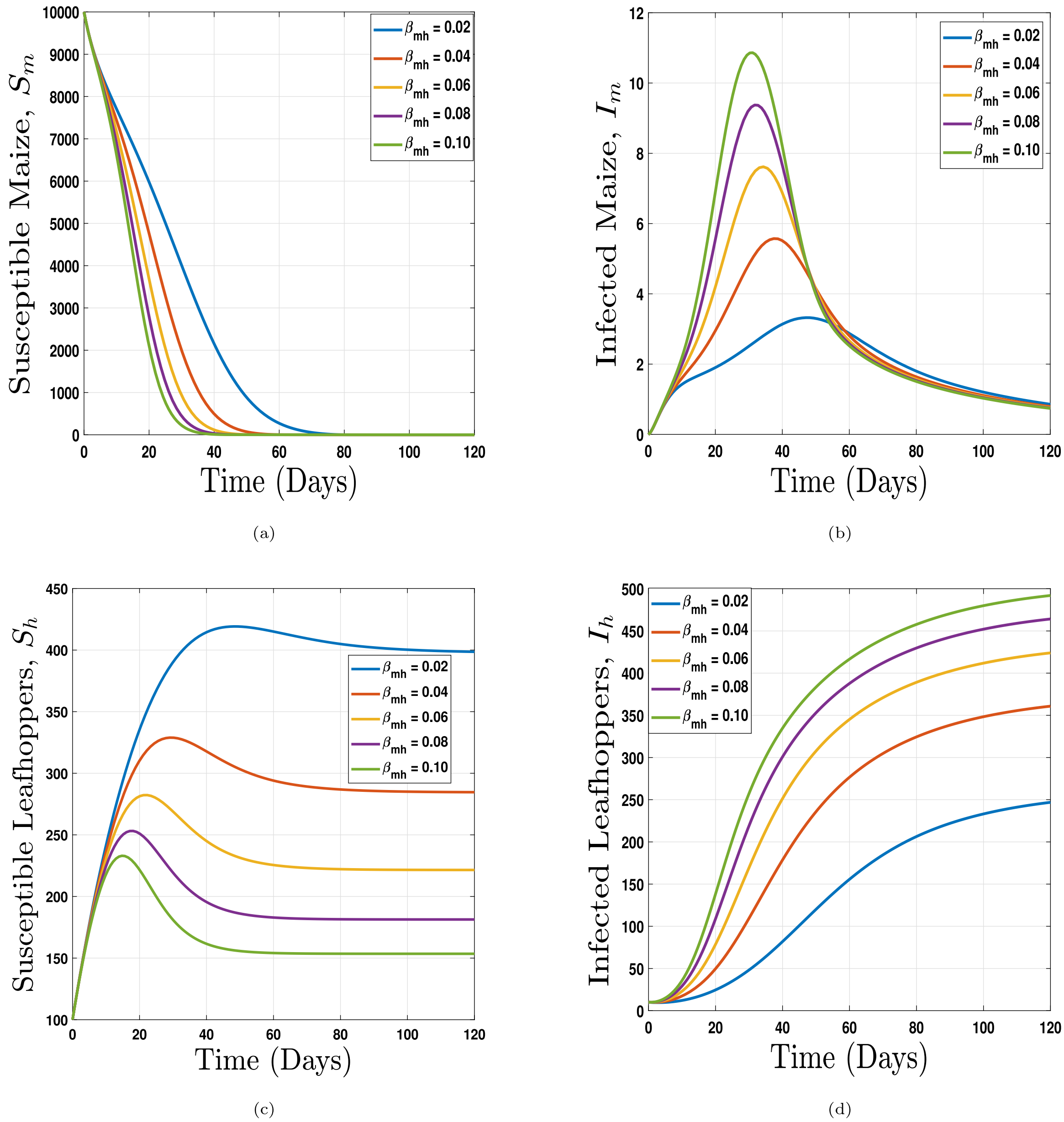

Fig. 3. Time Series plots of the effect of varying β_{mh}, the probability of Maize-to-Leafhopper transmission of MSVD.

Table 3
Cost and total maize infections averted for various control strategies.

Control strategy	Control combination	Total cost ($)	Total infected maize averted
1	u_1	692970	1082400
2	u_2	690800	−156870
3	u_3	691050	407290
4	u_4	692970	3201500
5	u_1, u_2	693700	905870
6	u_1, u_3	693060	2526000
7	u_1, u_4	695870	6300900
8	u_2, u_3	692270	244870
9	u_2, u_4	693690	3181300
10	u_3, u_4	694670	5412000
11	u_1, u_2, u_3	695150	2355500
12	u_1, u_2, u_4	696590	6286800
13	u_1, u_3, u_4	695220	6560800
14	u_2, u_3, u_4	695510	5402400
15	u_1, u_2, u_3, u_4	696050	6553100

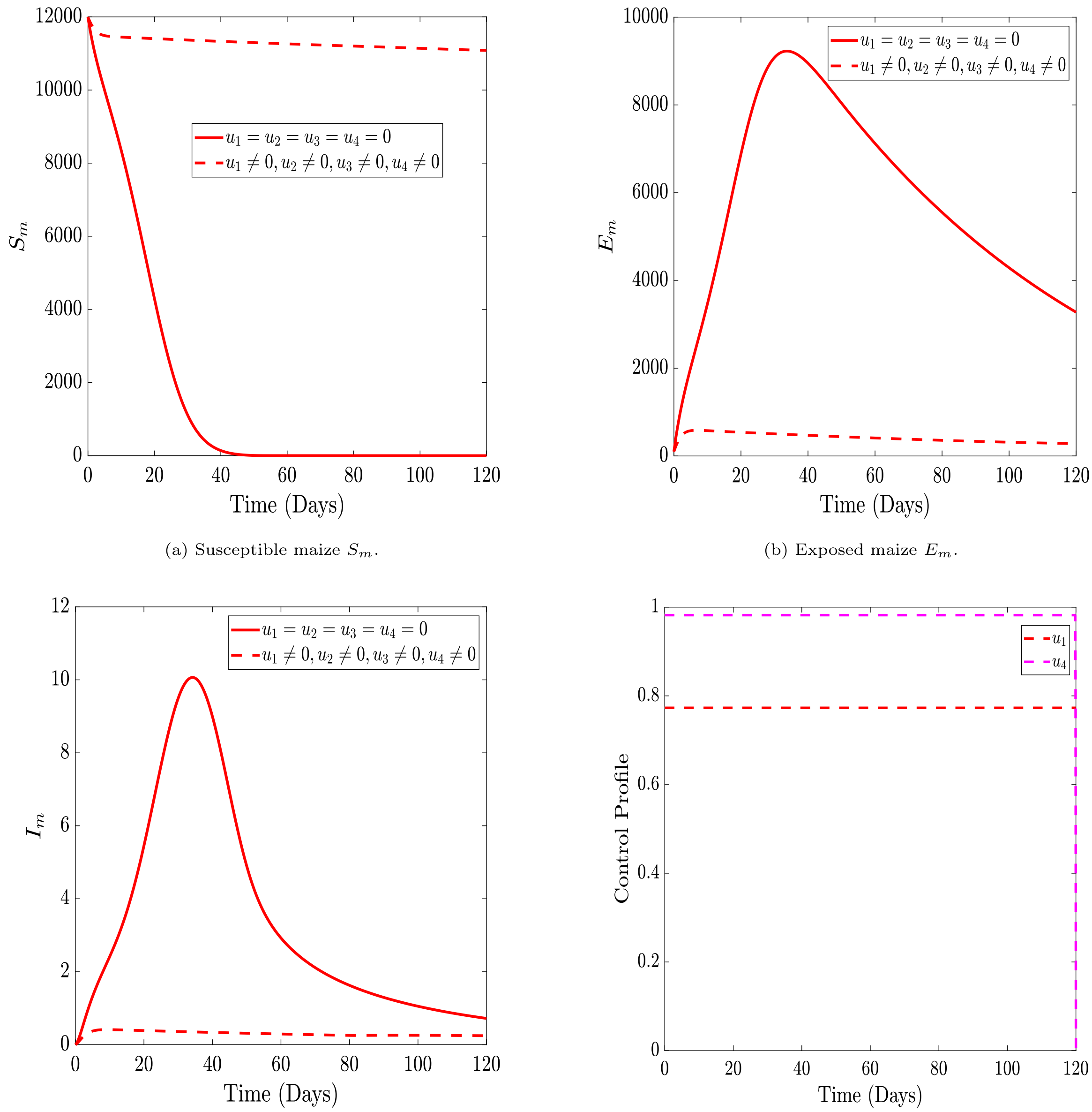

(a) Susceptible maize S_m.

(b) Exposed maize E_m.

(c) Infected maize I_m.

(d) Control profile for u_1 and u_4

Fig. 4. Optimal control simulation when one uses all the controls.

Incremental cost-effectiveness of single controls

The Control strategy 2 is not considered in the analysis because it does not avert infection of maize. The other strategies in this group are rated (CS_3, CS_1, CS_4) in increasing order of the total number of maize streak virus infections averted.

Control strategy	Control combination	Total cost ($)	Total infected maize Averted
1	u_1	692970	1082400
3	u_3	691050	407290
4	u_4	692970	3201500

The ICER of the various strategies are computed as follows:

ICER	Decision
$\text{ICER}(CS_3) = \frac{691050}{407290} = 1.696,$	
$\text{ICER}(CS_1, CS_3) = \frac{692970 - 691050}{1082400 - 407290} = 0.0028,$	CS_1 is better than CS_3,
$\text{ICER}(CS_1) = \frac{692970}{1082400} = 0.6402,$	
$\text{ICER}(CS_4, CS_1) = \frac{692970 - 692970}{3201500 - 1082400} = 0,$	CS_4 is better than CS_1.

Therefore, CS_4 (control for insecticide application to kill leafhoppers) is the most cost-effective single control strategy among the four strategies in Group A.

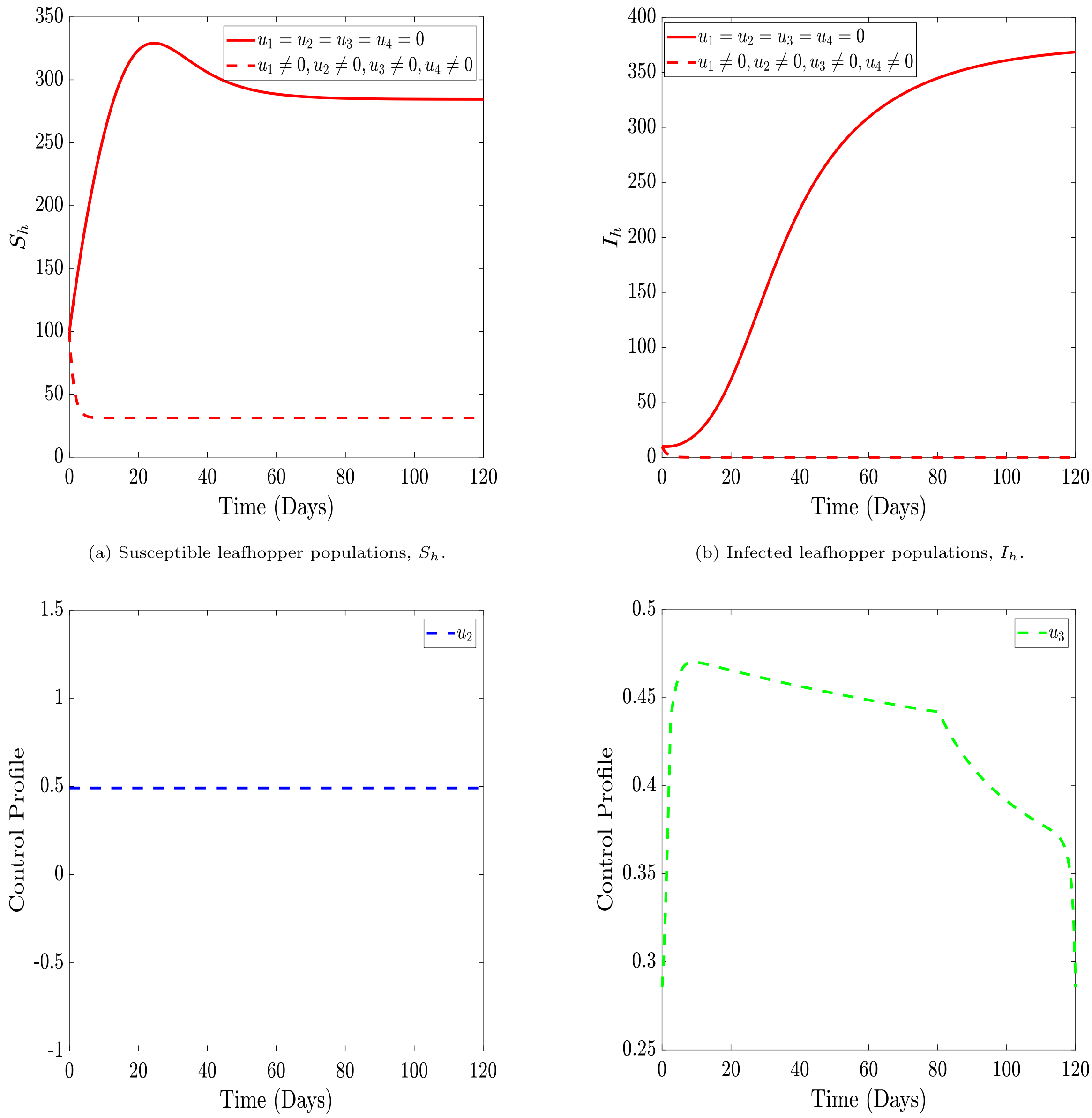

(a) Susceptible leafhopper populations, S_h.

(b) Infected leafhopper populations, I_h.

(c) Control profile for u_2

(d) Control profile for u_3

Fig. 5. Optimal control simulation when one use all the controls.

Incremental cost-effectiveness of double control combinations

The strategies in this group are also rated (CS_8, CS_5, CS_6, CS_9, CS_{10}, and CS_7) in increasing order of the total number of maize streak virus infections averted.

Control strategy	Control combination	Total cost ($)	Total infected maize Averted
8	u_2, u_3	692270	244870
5	u_1, u_2	693700	905870
6	u_1, u_3	693060	2526000
9	u_2, u_4	693690	3181300
10	u_3, u_4	694670	5412000
7	u_1, u_4	695870	6300900

The ICER are computed as follows:

ICER	Decision
$\text{ICER}(CS_8) = \frac{692270}{244870} = 2.8271,$	
$\text{ICER}(CS_5, CS_8) = \frac{693700 - 692270}{905870 - 244870} = 0.0022,$	CS_5 is better than CS_8
$\text{ICER}(CS_6, CS_5) = \frac{693060 - 693700}{2526000 - 905870} = -3.9503 \times 10^{-4},$	CS_6 is better than CS_5
$\text{ICER}(CS_9, CS_6) = \frac{693690 - 693060}{3181300 - 2526000} = 9.6139 \times 10^{-4},$	CS_6 is better than CS_9
$\text{ICER}(CS_{10}, CS_6) = \frac{694670 - 693060}{5412000 - 2526000} = 5.5787 \times 10^{-4},$	CS_{10} is better than CS_6
$\text{ICER}(CS_7, CS_{10}) = \frac{695870 - 694670}{6300900 - 5412000} = 0.0013$	CS_7 is better than CS_{10}.

Therefore, CS_7 (control for insecticide application to kill leafhoppers) is the most cost-effective among the four strategies in Group B.

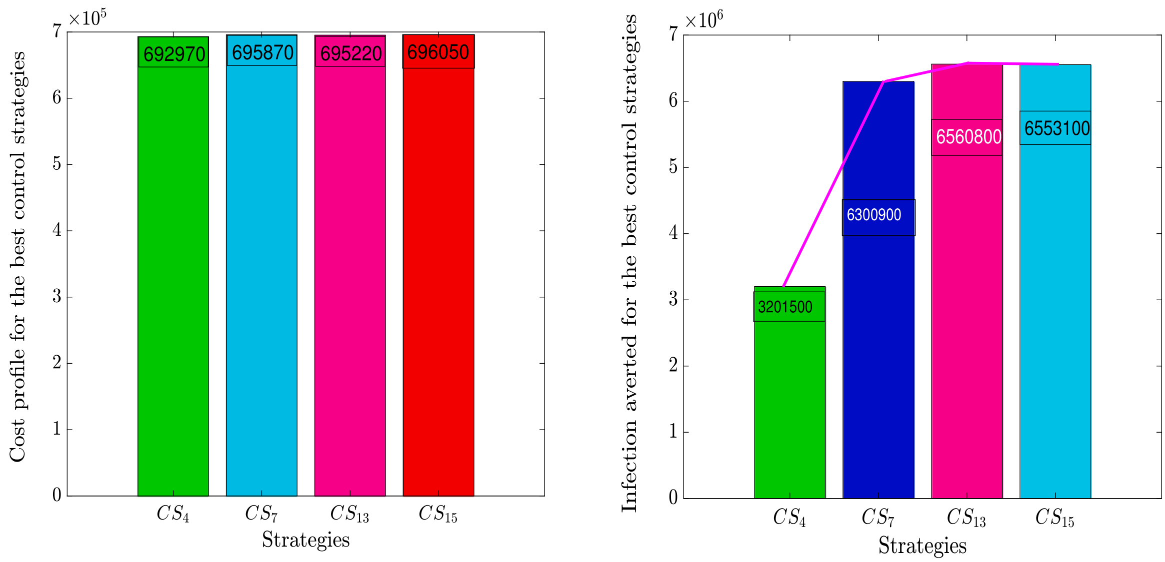

(a) Cost profile for best control strategies

(b) Infection Averted for the best control strategies

Fig. 6. Cost and benefit profiles of the best control strategies in the various groups.

Incremental cost-effectiveness of three control combinations

The strategies in this group are also rated (CS_{11}, followed by CS_{14}, CS_{12}, and CS_{13}) in increasing order of the total number of maize streak virus infections averted.

Control strategy	Control combination	Total cost ($)	Total infected maize Averted
11	u_1, u_2, u_3	695150	2355500
14	u_2, u_3, u_4	695510	5402400
12	u_1, u_2, u_4	696590	6286800
13	u_1, u_3, u_4	695220	6560800

The ICER are computed as follows:

ICER		Decision
ICER (CS_{11})	$= \frac{695150}{2355500} = 0.2951,$	
ICER (CS_{14}, CS_{11})	$= \frac{695510 - 695150}{5402400 - 2355500} = 1.1815 \times 10^{-4},$	CS_{14} is better than CS_{11}
ICER (CS_{14})	$= \frac{695510}{5402400} = 0.1287,$	
ICER (CS_{12}, CS_{14})	$= \frac{695510 - 695150}{5402400 - 2355500} = 1.1815 \times 10^{-4},$	CS_{12} is better than CS_{14}
ICER (CS_{12})	$= \frac{696590}{6286800} = 0.11080,$	
ICER (CS_{13}, CS_{12})	$= \frac{695220 - 696090}{6560800 - 6286800} = -0.0050$	CS_{13} is better than CS_{12}.

Therefore, CS_{13} (control for insecticide application to kill leafhoppers) is the most cost-effective among the four strategies in Group C.

Incremental cost-effectiveness among best strategies in all groups control combinations

Since Group D consists of only one strategy, CS_{15} is compared with the best from the other groups to determine the overall best strategy. These strategies are also arranged (CS_4, CS_7, CS_{15}, CS_{13}) in increasing order benefits.

Control strategy	Control combination	Total cost ($)	Total infected maize Averted
4	u_4	692970	3201500
7	u_1, u_4	695870	6300900
15	u_1, u_2, u_3, u_4	696050	6553100
13	u_1, u_3, u_4	695220	6560800

The ICER are calculated as follows:

ICER		Decision
ICER (CS_4)	$= \frac{692970}{3201500} = 0.2165$	
ICER (CS_7, CS_4)	$= \frac{695870 - 692970}{6300900 - 3201500} = 9.36 \times 10^{-4}$	CS_7 is better than CS_4
ICER (CS_7)	$= \frac{695870}{6300900} = 0.1104$	
ICER (CS_{13}, CS_7)	$= \frac{695220 - 695870}{6560800 - 6300900} = -0.0025$	CS_{13} is better than CS_7
ICER (CS_{13})	$= \frac{695220}{6560800} = 0.1060$	
ICER (CS_{15}, CS_{13})	$= \frac{696050 - 695220}{6553100 - 6560800} = -0.1078$	CS_{15} is better than CS_{13}

Therefore, the overall most cost-effective strategy is CS_{15} which involves the implementation of all four controls. The simulation results depicting the relative effect of implementing the best control strategy are presented in Figs. 4and Fig. 5.

Figs. 6(a) and 6(b) show the control cost profile and infection averted profile for the best control strategies.

Conclusions

This paper offered a mathematical analysis of maize streak virus disease transmission dynamics using Holling's Type II predation form and standard incidence. Thus, to better understand the disease's transmission and to look into feasible prevention and control techniques to stop the infection from spreading. The sensitivity analysis of the MSVD model reveals that β_{mh}, the likelihood of MSVD transmission from infected maize plant to susceptible leafhopper, is the most positive sensitivity parameter, followed by β_{hm}, the probability of MSVD transmission from infected leafhopper to maize plants. We also discovered that b, the rate of inflow of susceptible leafhoppers, is the most negative sensitivity parameter, followed by a, the infected leafhopper conversion rate. We incorporated four time-dependent control variables into the model using the sensitivity analysis results. We used cost-effectiveness analysis to evaluate the advantages of various control tactics and offer ways to manage infections using the incremental cost-effectiveness ratio. The optimal control analysis shows that the most efficient control technique uses all four control variables.

Declaration of competing interest

The authors declare that they have no known competing financial interests or personal relationships that could have appeared to influence the work reported in this paper.

Data availability

No data was used for the research described in the article.

Acknowledgement

All authors read and approved the final manuscript.

References

[1] FAO. Crops and livestock products. 2016.
[2] FAO. International Year of Plant Health – Final report. Food and Agricultural Organization of the United Nations; 2021.
[3] Pratt RC, Gordon SG. Breeding for resistance to maize foliar pathogens. In: Plant breeding reviews. John Wiley & Sons, Inc.; 2010, p. 119–73. http://dx.doi.org/10.1002/9780470650349.ch3.
[4] Asamoah JKK, Owusu MA, Jin Z, Oduro F, Abidemi A, Gyasi EO. Global stability and cost-effectiveness analysis of COVID-19 considering the impact of the environment: using data from ghana. Chaos Solitons Fractals 2020;140:110103.
[5] Omame A, Nnanna C, Inyama S. Optimal control and cost-effectiveness analysis of an HPV–Chlamydia trachomatis co-infection model. Acta Biotheoret 2021;69(3):185–223.
[6] Olaniyi S. Dynamics of Zika virus model with nonlinear incidence and optimal control strategies. Appl Math Inf Sci 2018;12(5):969–82.
[7] Asamoah JKK, Yankson E, Okyere E, Sun G-Q, Jin Z, Jan R, et al. Optimal control and cost-effectiveness analysis for dengue fever model with asymptomatic and partial immune individuals. Results Phys 2021;31:104919.
[8] Ali N, Nawaz R, Zada L, Mouldi A, Bouzgarrou SM, Sene N. Analytical approximate solution of the fractional order biological population model by using natural transform. J Nanomater 2022;2022.
[9] Agusto FB, Adekunle A. Optimal control of a two-strain tuberculosis-HIV/AIDS co-infection model. Biosystems 2014;119:20–44.
[10] Asamoah JKK, Jin Z, Sun G-Q, Seidu B, Yankson E, Abidemi A, Oduro F, Moore SE, Okyere E. Sensitivity assessment and optimal economic evaluation of a new COVID-19 compartmental epidemic model with control interventions. Chaos Solitons Fractals 2021;146:110885.
[11] Agusto F, Leite M. Optimal control and cost-effective analysis of the 2017 meningitis outbreak in Nigeria. Infectious Disease Modelling 2019;4:161–87.
[12] Seidu B, Makinde OD. Optimal control of HIV/AIDS in the workplace in the presence of careless individuals. Comput Math Methods Med 2014;2014.
[13] Sene N. Analysis of the stochastic model for predicting the novel coronavirus disease. Adv Difference Equ 2020;2020(1):1–19.
[14] Seidu B. Optimal strategies for control of COVID-19: A mathematical perspective. Scientifica 2020;2020.
[15] Munusamy K, Ravichandran C, Nisar KS, Ghanbari B. Existence of solutions for some functional integrodifferential equations with nonlocal conditions. Math Methods Appl Sci 2020;43(17):10319–31.
[16] Ghanbari B, Nisar KS. Determining new soliton solutions for a generalized nonlinear evolution equation using an effective analytical method. Alex Eng J 2020;59(5):3171–9.
[17] Kumar P, Erturk VS, Nisar KS, Jamshed W, Mohamed MS. Fractional dynamics of 2019-nCOV in Spain at different transmission rate with an idea of optimal control problem formulation. Alex Eng J 2022;61(3):2204–19.
[18] Addai E, Zhang L, Ackora-Prah J, Gordon JF, Asamoah JKK, Essel JF. Fractal-fractional order dynamics and numerical simulations of a Zika epidemic model with insecticide-treated nets. Physica A 2022;127809.
[19] Nisar KS, Logeswari K, Vijayaraj V, Baskonus HM, Ravichandran C. Fractional order modeling the gemini virus in capsicum annuum with optimal control. Fract Fraction 2022;6(2):61.
[20] Zada I, Naeem Jan M, Ali N, Alrowail D, Sooppy Nisar K, Zaman G. Mathematical analysis of hepatitis B epidemic model with optimal control. Adv Difference Equ 2021;2021(1):1–29.
[21] Abidemi A, Ackora-Prah J, Fatoyinbo HO, Asamoah JKK. Lyapunov stability analysis and optimization measures for a dengue disease transmission model. Physica A 2022;127646.
[22] Khater MM, Ghanbari B, Nisar KS, Kumar D. Novel exact solutions of the fractional Bogoyavlensky–Konopelchenko equation involving the Atangana-Baleanu-Riemann derivative. Alex Eng J 2020;59(5):2957–67.
[23] Hussain T, Ozair M, Faizan M, Jameel S, Nisar KS. Optimal control approach based on sensitivity analysis to retrench the pine wilt disease. Eur Phys J Plus 2021;136(7):1–27.
[24] Abidemi A, Fatoyinbo HO, Asamoah JKK. Analysis of dengue fever transmission dynamics with multiple controls: a mathematical approach. In: 2020 international conference on decision aid sciences and application (DASA). IEEE; 2020, p. 971–8.
[25] Asamoah JKK, Jin Z, Sun G-Q, Li MY. A deterministic model for Q fever transmission dynamics within dairy cattle herds: using sensitivity analysis and optimal controls. Comput Math Methods Med 2020;2020.
[26] Asamoah JKK. Fractal–fractional model and numerical scheme based on Newton polynomial for Q fever disease under Atangana–Baleanu derivative. Results Phys 2022;34:105189.
[27] Asamoah JKK, Okyere E, Yankson E, Opoku AA, Adom-Konadu A, Acheampong E, Arthur YD. Non-fractional and fractional mathematical analysis and simulations for q fever. Chaos Solitons Fractals 2022;156:111821.
[28] Omame A, Isah ME, Abbas M, Abdel-Aty A-H, Onyenegecha CP. A fractional order model for dual variants of COVID-19 and HIV co-infection via Atangana-Baleanu derivative. Alex Eng J 2022;61(12):9715–31.
[29] Sun G-Q, Li M-T, Zhang J, Zhang W, Pei X, Jin Z. Transmission dynamics of brucellosis: Mathematical modelling and applications in China. Comput Struct Biotechnol J 2020;18:3843–60.
[30] Nazir A, Ahmed N, Khan U, Mohyud-Din ST, Nisar KS, Khan I. An advanced version of a conformable mathematical model of Ebola virus disease in Africa. Alex Eng J 2020;59(5):3261–8.
[31] Ali A, Iqbal Q, Asamoah JKK, Islam S. Mathematical modeling for the transmission potential of Zika virus with optimal control strategies. Eur Phys J Plus 2022;137(1):1–30.
[32] Kumar P, Erturk VS, Abboubakar H, Nisar KS. Prediction studies of the epidemic peak of coronavirus disease in Brazil via new generalised Caputo type fractional derivatives. Alex Eng J 2021;60(3):3189–204.
[33] Acheampong E, Okyere E, Iddi S, Bonney JH, Asamoah JKK, Wattis JA, Gomes RL. Mathematical modelling of earlier stages of COVID-19 transmission dynamics in Ghana. Results Phys 2022;34:105193.
[34] Ma X, Luo X-F, Li L, Li Y, Sun G-Q. The influence of mask use on the spread of COVID-19 during pandemic in New York City. Results Phys 2022;34:105224.
[35] Rwezaura H, Diagne M, Omame A, de Espindola A, Tchuenche J. Mathematical modeling and optimal control of SARS-CoV-2 and tuberculosis co-infection: a case study of Indonesia. Model Earth Syst Environ 2022;1–28.
[36] Collins KJ. Optimal control of maize foliar diseases using the plants population dynamics. Acta Agricult Scand B - Soil Plant Sci 2016;66:20–6. http://dx.doi.org/10.1080/09064710.2015.1061588.
[37] Aloyce W, Kuznetsov D, et al. A mathematical model for the mlnd dynamics and sensitivity analysis in a maize population. Asian J Math Appl 2017.
[38] Alemneh HT, Makinde OD, Theuri DM. Ecoepidemiological model and analysis of MSV disease transmission dynamics in Maize plant. Int J Math Math Sci 2019;2019:1–14. http://dx.doi.org/10.1155/2019/7965232.
[39] Alemneh HT, Makinde OD, Theuri DM. Optimal control model and cost effectiveness analysis of Maize streak virus pathogen interaction with pest invasion in Maize plant. Egypt J Basic Appl Sci 2020;7(1):180–93. http://dx.doi.org/10.1080/2314808x.2020.1769303.
[40] Alemneh HT, Kassa AS, Godana AA. An optimal control model with cost effectiveness analysis of Maize streak virus disease in maize plant. Infect Dis Model 2021;6:169–82.
[41] Asamoah JKK, Bornaa C, Seidu B, Jin Z. Mathematical analysis of the effects of controls on transmission dynamics of SARS-CoV-2. Alex Eng J 2020;59(6):5069–78.
[42] Yang X, Chen L, Chen J. Permanence and positive periodic solution for the single-species nonautonomous delay diffusive models. Comput Math Appl 1996;32(4):109–16.
[43] van den Driessche P, Watmough J. Reproduction numbers and sub-threshold endemic equilibria for compartmental models of disease transmission. Math Biosci 2002;180(1):29–48. http://dx.doi.org/10.1016/S0025-5564(02)00108-6.
[44] Asamoah JKK, Oduro FT, Bonyah E, Seidu B. Modelling of rabies transmission dynamics using optimal control analysis. J Appl Math 2017;2017.
[45] Castillo-Chavez B. Dynamical models of tuberculosis and their applications. Math Biosci Eng 2004;1:361–404. http://dx.doi.org/10.3934/mbe.2004.1.361.
[46] Lenhart S, Workman JT. Optimal control applied to biological models. Chapman and Hall/CRC; 2007.
[47] Fleming W, Rishel R. Optimal control of Markov diffusion processes. In: Deterministic and stochastic optimal control. Springer New York; 1975, p. 151–97. http://dx.doi.org/10.1007/978-1-4612-6380-7_6.

[48] Pontryagin LS. The mathematical theory of optimal processes. vol. 4, CRC Press; 1962.
[49] Bosque-Pérez NA. Eight decades of maize streak virus research. Virus Res 2000;71(1–2):107–21.
[50] MAIZE: HArvesting period: In general, maize requires 120 days (12 weeks) to reach maturity. However, early maturing varieties take 75-80 days. 2021, http://gis4agricgh.net/POLICIES/commodities/Commodity.
[51] BioNet-Eatrinet. Cicadulina mbila (naude)-maize leafhopper. 2021, https://keys.lucidcentral.org/keys/v3/eafrinet/maize_pests/key/maize_pests/Media/Html/Cicadulina_mbila_(Naude)_-_Maize_Leafhopper.htm.
[52] Alemneh HT, Makinde OD, Mwangi Theuri D. Ecoepidemiological model and analysis of MSV disease transmission dynamics in maize plant. Int J Math Math Sci 2019;2019.
[53] Alemneh HT, Makinde OD, Theuri DM. Mathematical modelling of msv pathogen interaction with pest invasion on maize plant. Glob J Pure Appl Math 2019;15(1):55–79.
[54] Abidemi A, Aziz NAB. Optimal control strategies for dengue fever spread in Johor, Malaysia. Comput Methods Programs Biomed 2020;196:105585.
[55] Asamoah JKK, Jin Z, Sun G-Q. Non-seasonal and seasonal relapse model for Q fever disease with comprehensive cost-effectiveness analysis. Results Phys 2021;22:103889.
[56] Asamoah JKK, Okyere E, Abidemi A, Moore SE, Sun G-Q, Jin Z, Acheampong E, Gordon JF. Optimal control and comprehensive cost-effectiveness analysis for COVID-19. Results Phys 2022;105177.